Part II. Viscous Flow Around Circulating Spheres of Low Viscosity

A. E. HAMIELEC, A. I. JOHNSON, and W. T. HOUGHTON

McMaster University, Hamilton, Ontario, Canada

Steady state solutions of the Navier-Stokes equations for Reynolds numbers of 0.1, 1, 50, 100, and 200 have been obtained by using finite-difference methods. The effects of radial and angular step size and wall proximity have been investigated. Results were found in the form of stream function and vorticity distributions with pressure distributions and drag coefficients calculated from them. The results compare favorably with experimental data and show a steady trend from Hadamard-Rybczynski flow to boundary-layer flow after Levich-Chao-Moore. For a circulating sphere of low viscosity there is no flow separation indicated at Reynolds numbers equal to or less than 200.

The Navier-Stokes equation has proved insoluble for the problem of axisymmetric flow around spherical gas bubbles or drops of low viscosity, except by methods which first linearize the equations [Hadamard-Rybczynski solution (*1, 2*)], error-distribution methods which require tedious algebra [Hamielec et al. (*3*)], and boundary-layer methods which apply only when $N_{Re} >> 1$ [Levich-Chao-Moore (*4* to *6*) and Conkie and Savic (*7*)].

A finite-difference method was used by Jenson (*8*) to solve the Navier-Stokes equation for flow around a solid sphere for Reynolds numbers of 5, 10, 20, and 40. Jenson used relaxation techniques and a desk calculator. In the present study the methods of Jenson are closely followed. The present solutions were obtained by using an iterative procedure to solve the finite-difference equations with IBM 7040 and 7094 computers.

THEORY

The Navier-Stokes equation for viscous, incompressible, axisymmetric flow for the stream function Ψ in spherical polars may be written as

$$\frac{N_{Re}}{2}\left[\frac{\partial\Psi}{\partial r}\frac{\partial}{\partial\theta}\left(\frac{E^2\Psi}{r^2\sin^2\theta}\right) - \frac{\partial\Psi}{\partial\theta}\frac{\partial}{\partial r}\left(\frac{E^2\Psi}{r^2\sin^2\theta}\right)\right]\sin\theta = E^4\Psi \qquad (1)$$

Equation (1) may be split into two simultaneous second-order equations by introducing the vorticity ζ as follows:

$$E^2\Psi = \zeta r\sin\theta \qquad (2)$$

$$\frac{N_{Re}}{2}\left[\frac{\partial\Psi}{\partial r}\frac{\partial}{\partial\theta}\left(\frac{\zeta}{r\sin\theta}\right) - \frac{\partial\Psi}{\partial\theta}\frac{\partial}{\partial r}\left(\frac{\zeta}{r\sin\theta}\right)\right]\sin\theta = E^2(\zeta r\sin\theta) \qquad (3)$$

All quantities have been made dimensionless by putting

$$r = \frac{r^1}{A},\quad \Psi = \frac{\Psi^1}{UA^2},\quad \zeta = \frac{\zeta^1 A}{U},\quad N_{Re} = \frac{2UA}{\nu}$$

Following Jenson, an exponential step size in the radial direction is used, by employing the substitution $r = e^Z$ and taking equal intervals in Z. The stream function and vorticity vary most rapidly near the sphere surface and hence it is desirable to have a small step size at the surface. Because the core storage of digital computers is a limiting factor in the solution of problems where the boundaries are infinite, the exponential step size plays an important role in reducing the number of mesh points. Equations (2) and (3) become

$$e^{2Z}\,E^2\Psi - \zeta e^{3Z}\sin\theta = 0 \qquad (4)$$

$$\frac{N_{Re}}{2}\left[\frac{\partial\Psi}{\partial Z}\frac{\partial F}{\partial\theta} - \frac{\partial\Psi}{\partial\theta}\frac{\partial F}{\partial Z}\right]e^Z\sin\theta - e^{2Z}E^2G = 0 \qquad (5)$$

where

$$e^{2Z}E^2 = \frac{\partial^2}{\partial Z^2} - \frac{\partial}{\partial Z} + \sin\theta\frac{\partial}{\partial\theta}\left(\frac{1}{\sin\theta}\frac{\partial}{\partial\theta}\right)$$

$$F = \zeta/e^Z\sin\theta,\quad G = \zeta e^Z\sin\theta$$

Considering lattice spacing A in the Z direction and B in the θ direction, Equations (4) and (5) take the following finite-difference form (see Figure 1† and reference 8):

$$\Psi(I,J+1)\left(\frac{2-A}{2A^2}\right) + \Psi(I,J-1)\left(\frac{2+A}{2A^2}\right) + \Psi(I+1,J)\left(\frac{2-B\cot\theta(I)}{2B^2}\right) + \Psi(I-1,J)\left(\frac{2+B\cot\theta(I)}{2B^2}\right) - \Psi(I,J)\left(\frac{2}{A^2}+\frac{2}{B^2}\right) - G(I,J)e^{2Z(J)} = 0 \qquad (6)$$

$$G(I,J+1)\left(\frac{2-A}{2A^2}\right) + G(I,J-1)\left(\frac{2+A}{2A^2}\right) + G(I+1,J)\left(\frac{2-B\cot\theta(I)}{2B^2}\right) + G(I-1,J)\left(\frac{2+B\cot\theta(I)}{2B^2}\right) - G(I,J)\left(\frac{2}{A^2}+\frac{2}{B^2}\right) - \frac{N_{Re}}{4}e^{Z(J)}\sin\theta(I)\left[\left(\frac{\Psi(I,J+1)-\Psi(I,J-1)}{2A}\right)\left(\frac{F(I+1,J)-F(I,-1,J)}{B}\right) - \left(\frac{\Psi(I+1,J)-\Psi(I-1,J)}{2B}\right)\left(\frac{F(I,J+1)-F(I,J-1)}{A}\right)\right] = 0 \qquad (7)$$

† Figure 1 appears in Part I, page 213.

In the iterative procedure to solve Equations (6) and (7) relaxation factors were used to stabilize the computations. They were introduced as follows:

$$\Psi_n(I,J) = \Psi_{n-1}(I,J) + WW[\Psi_n^*(I,J) - \Psi_{n-1}(I,J)] \tag{8}$$

$$G_n(I,J) = G_{n-1}(I,J) + W[G_n^*(I,J) - G_{n-1}(I,J)] \tag{9}$$

where the subscript n denotes the n^{th} value calculated and the asterisk denotes the value calculated by using Equations (6) and (7). Starting values for Ψ and G were obtained from analytical solutions. At low Reynolds numbers the Hadamard-Rybczynski solution was used, giving

$$\Psi = \left(\frac{1}{2}r^2 - 0.5r\right)\sin^2\theta \tag{10}$$

$$\zeta = \frac{1}{r^2}\sin\theta \tag{11}$$

At high Reynolds numbers the potential flow solution was used, giving

$$\Psi = \left(\frac{1}{2}r^2 - 0.5/r\right)\sin^2\theta \tag{12}$$

$$\zeta = 0 \tag{13}$$

When solving Equations (2) and (3) or (6) and (7), boundary conditions are required which specify all values of Ψ and ζ or Ψ and G on a boundary completely enclosing the region of flow. The boundary conditions for Ψ are:

for $\theta = 0°$	$\Psi = 0$	axis of symmetry
$\theta = 180°$	$\Psi = 0$	axis of symmetry
$Z = 0$	$\Psi = 0$	surface of sphere

To complete the boundary, the disturbance caused by the sphere was set equal to zero at a concentric spherical boundary moving with the sphere. The position of the boundary was varied to investigate the effect of wall proximity. The stream function for parallel flow is:

$$\Psi = \frac{1}{2}e^{2Z}\sin^2\theta$$

The boundary conditions for ζ are:

for $\theta = 0°$	$\zeta = 0$	axis of symmetry
$\theta = 180°$	$\zeta = 0$	axis of symmetry

For parallel flow the vorticity is zero. The vorticity at the surface of the spherical bubble was determined from the condition of zero tangential stress at the surface, that is

$$\frac{\partial V_\theta}{\partial r} - V_\theta = 0$$

Now

$$\zeta = \frac{\partial V_\theta}{\partial r} + V_\theta$$

$$\therefore \zeta = 2V_\theta$$

and since $V_\theta = \dfrac{1}{\sin\theta}\dfrac{\partial\Psi}{\partial r}$

$$\therefore \zeta = \frac{2}{\sin\theta}\frac{\partial\Psi}{\partial r}$$ at the surface of the fluid sphere.

This may be written in finite-difference form as

$$\zeta(I,1) = \frac{1}{\sin\theta(I)}\left(\frac{4\Psi(I,2) - \Psi(I,3)}{A}\right) \tag{14}$$

Along the first line of lattice points at $\theta = B$, special treatment is needed for the term $\dfrac{G(I-1,J)}{\sin\theta(I-1)}$ in Equation (7), because although $G(1,J) = 0$, $\sin\theta(1) = 0$ also. L'Hopital's rule may be used to give

$$\frac{G(1,J)}{\sin(1)} = \frac{G(2,J)}{B}$$

A similar correction is necessary on the last row of lattice points at the rear of the sphere. The calculations are started by using initially guessed values of Ψ and G to calculate an improved Ψ by using Equation (6). The new Ψ found with the relaxation factor WW in Equation (8) is substituted into Equation (7) to find an improved G. The new G found with the relaxation factor W in Equation (9) is now substituted into Equation (6) and this procedure is repeated until Ψ and G change by less than a specified tolerance per iteration. The tolerance chosen for all calculations was 0.0001 for both Ψ and G.

The pressure distribution on the fluid-fluid interface may be calculated as follows. One component of the Navier-Stokes equation reduces to

$$\frac{\partial P}{\partial\theta} = \frac{4}{N_{Re}}\left[\frac{\partial\zeta}{\partial r} + \zeta\right] - 2V_\theta\frac{\partial V_\theta}{\partial\theta} \tag{15}$$

Integrating one obtains

$$P - P_o = \frac{4}{N_{Re}}\int_o^\theta\left(\frac{\partial\zeta}{\partial r} + \zeta\right)d\theta - V_\theta^2 \tag{16}$$

On the fluid-fluid interface

$$V_\theta = 0.5\ \zeta \tag{17}$$

$$\therefore P - P_o = \frac{4}{N_{Re}}\int_o^\theta\left(\frac{\partial\zeta}{\partial r} + \zeta\right)d\theta - 0.25\zeta^2 \tag{18}$$

It may readily be shown (8) that

$$P_o = 1 + \frac{8}{N_{Re}}\int_1^\infty\left(\frac{\partial\zeta}{\partial\theta}\right)\frac{dr}{r} \tag{19}$$

where $(\partial\zeta/\partial\theta)$ is evaluated along the line $\theta = 0$.

Equations (18) and (19) were then written in finite-difference form and used to calculate the pressure distribution on the surface of the fluid sphere.

The following drag coefficient formulas were used:

$$C_{DF} = \frac{4}{N_{Re}}\int_o^\pi\left(\frac{\partial\zeta}{\partial\theta} + \zeta\cot\theta\right)\sin 2\theta d\theta \tag{20}$$

$$C_{DP} = \int_o^\pi P\sin 2\theta d\theta \tag{21}$$

ANALYTIC SOLUTION

An analytic solution has been found for creeping flow whose boundary conditions are identical to those used in the finite-difference method. This solution is

$$\Psi = (A/r + Br + Cr^2 + Dr^4)\sin^2\theta \tag{22}$$

The constants are found by satisfying the boundary conditions

$$r = 1\ \Psi = o,\ \tau_{r\theta} = 0$$

$$r = R\ \Psi = \frac{1}{2}R^2\sin^2\theta,\ \zeta = 0 \tag{23}$$

The constants are given by the relationships

$$B = \frac{5/2R^6}{(-5R^6 + 6R^5 - 1)} \tag{24}$$

$$C = -B \tag{25}$$

$$D = \frac{1/2R^3}{(-5R^6 + 6R^5 - 1)} \tag{26}$$

$$A = -D \tag{27}$$

The total drag coefficient is given by

$$C_D = \frac{-32B}{Re} \tag{28}$$

RESULTS

Detailed results of interest are available elsewhere.† These include the radial and angular step sizes, the position of the outer spherical boundary, surface vorticity and pressure distributions, and form and friction drag coefficients. To reduce the size of the tables of computed results and yet to present as much useful data as possible, only surface values of vorticity and pressure have been tabulated. If a complete knowledge of the vorticity and stream function throughout the flow field is required a computer deck containing this information will be provided by A. E. Hamielec.

Graphs of surface vorticity and pressure distribution showing the effect of varying the Reynolds number are presented in Figures 2 and 3. Also shown in Figure 3 is the pressure distribution for potential flow for comparison.

Table 1 illustrates the effect of varying the position of the outer spherical boundary on the total drag coefficient. Predictions of the analytical solutions after Satapathy et al. (9) and of the present investigation are compared with the finite-difference solutions.

In Table 2 a comparison is made of a boundary-layer solution after Moore (6) and finite-difference solutions with an experimental correlation after Tadaki and Maeda (10). Predicted and measured total drag coefficients are compared.

† Deposited as document 9158 with the American Documentation Institute, Photoduplication Service, Library of Congress, Washington 25, D. C., and may be obtained for $2.50 for photoprints or $1.75 for 35-mm. microfilm.

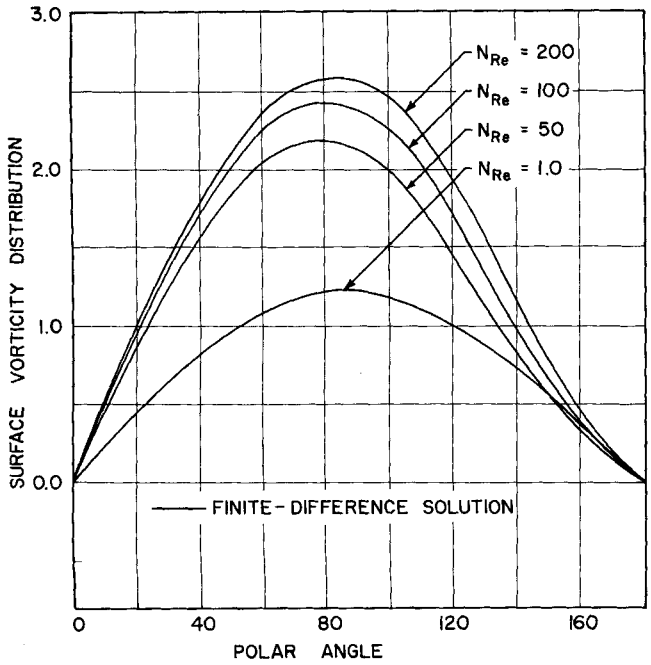

Fig. 2. Surface vorticity distribution; finite-difference solution.

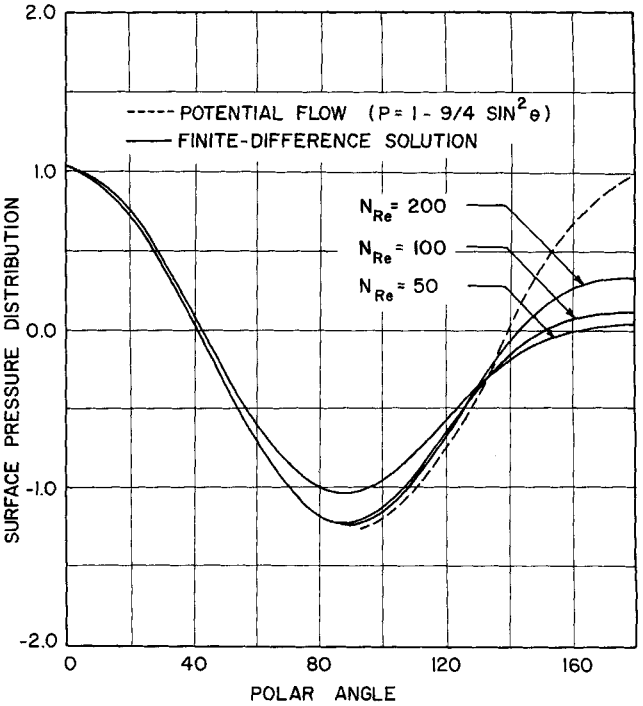

Fig. 3. Surface pressure distribution; finite-difference solution and potential flow.

DISCUSSION OF RESULTS

Accuracy of Solutions

The accuracy of the finite-difference solutions has been examined by varying the radial and angular step sizes and by comparing predicted quantities with those of limiting analytical solutions. These include solutions after Hadamard-Rybczynski (1, 2), Levich-Chao-Moore (4 to 6) and the analytical solution developed in this investigation.

There are several considerations which must be made when choosing the optimum step sizes. The step sizes and position of the outer boundary must be chosen to eliminate or reduce to an insignificant level oscillation of the vorticity (or G) near the outer boundary. Such oscillation can cause the solutions to become unstable if very small relaxation factors are not used. These small relaxation factors lead to excessively long computation times. The following argument after Jenson (8) may be used to establish criteria for estimating radial and angular step sizes to eliminate such oscillations:

Table 1. Wall Effects and Applicability of Linearized Equations of Motion
$N_{Re} = 0.1$

Position of outer boundary (dimensionless)	Satapathy et al. (9)	Total drag coefficient Present results Equation (22)	Finite difference
2.01	536	397	390
3.86	261	232	230
7.05	203	192	192
12.25	182	178	183
19.14	174	172	176
∞	160	160	—

TABLE 2. COMPARISON OF BOUNDARY-LAYER THEORY WITH FINITE-DIFFERENCE METHOD

N_{Re}	Experimental correlation after Tadaki and Maeda (*10*)	Total drag coefficient: Moore's results (*6*)	Total drag coefficient: Present results
50	0.75	0.66	0.71
100	0.42	0.38	0.40
200	0.24	0.20	0.27

$$\Delta Res\ (I, J+1) = \left(\frac{2+A}{2A^2}\right)\ (e^{Z(J)} \sin\theta(I)) - \frac{N_{Re}}{4A}\ \frac{\partial\psi}{\partial\theta}\ (I, J+1)\ \frac{e^{Z(J+1)}}{e^{Z(J)}} \qquad (29)$$

Equation (29) gives the change in the residual ΔRes at point $(I, J+1)$ caused by a unit change in ζ at point (I, J). By using the potential flow model to calculate $(\partial\psi/\partial\theta)$ and assuming the $A << 1$, Equation (29) becomes

$$\Delta Res\ (I, J+1) = \left(\frac{e^{Z(J)}\sin\theta(I)}{A}\right) \left(\frac{1}{A} + \frac{N_{Re}\cos\theta(I)}{4e^{2Z(J)}} - \frac{N_{Re}\, e^{Z(J)}}{4}\cos(I)\right) \qquad (30)$$

and similarly

$$\Delta Res\ (I-1, J) = \frac{2e^{Z(J)}\sin\theta(I) - Be^{Z(J)}\cos\theta(I)}{2B^2} - \frac{N_{Re}}{4B}\left(e^{2Z(J)} + \frac{e^{-Z(J)}}{2}\right)\sin^2\theta(I) \qquad (31)$$

If $\Delta Res\ (I, J+1)$ or $\Delta Res\ (I-1, J)$ is negative, the vorticity or G at these points will be of opposite sign to that at point (I, J) and the result will be oscillating values of vorticity or G. The value of A and B must be chosen to keep $\Delta Res\ (I, J+1)$ and $\Delta Res\ (I-1, J)$ positive. To prevent oscillating values at the outer boundary, A must be chosen as follows:

$$A < \frac{4}{N_{Re}\, e^{Z(J)}} \qquad (32)$$

and similarly

$$B < \frac{4}{N_{Re}\, e^{Z(J)}} \qquad (33)$$

Equations (29) to (33) were used as a guide. However, these criteria were found to be overly conservative and had they been strictly adhered to they would have led to excessively long computation. In the present study these minimum values of A and B were exceeded with the result that for the computations at the larger Reynolds numbers some oscillating values of the vorticity were found near the outer boundary downstream from the sphere. However, for all Reynolds numbers investigated there was no evidence found of oscillation at the sphere surface. Care was taken when choosing A, B, and N to reduce this oscillation near the outer boundary to an insignificant level.

Two levels of step size for both radial and angular directions were used in the finite-difference solutions. These included angular step sizes of 3 and 6 deg. and radial step sizes of $A = 0.025$ and 0.05. A combination of a 3-deg. angular step size and $A = 0.025$ would have required a long computation time and therefore was not attempted. We believe that the largest error in the finite-difference solutions is probably due to the presence of the outer spherical boundary at a finite distance from the sphere surface. Errors due to the finite step sizes chosen are considered unimportant except perhaps for the solution at $N_{Re} = 200$.

COMPARISON OF THE FINITE-DIFFERENCE METHOD WITH OTHER THEORIES

Satapathy et al. (9) have generalized the Hadamard-Rybczynski theory to allow for a finite, spherical outer boundary. They used solutions to the linearized equations of motion and put the disturbance to parallel flow caused by the fluid sphere as zero on a concentric spherical boundary moving with the sphere. It should be mentioned that they did not set the vorticity to zero on the outer boundary. However, as $R \to \infty$ this condition is also satisfied. In the present study the boundary conditions for the analytic solution and for the finite-difference solutions are identical. For large values of R they become identical with Satapathy's solution as well. A comparison of predicted drag coefficients for these three solutions is made in Table 1. The agreement of the finite-difference method with analytic solution [Equation (22)] is satisfactory. This suggests that deviations of experimental data for an infinite fluid are principally due to wall effects and not to errors inherent in the finite-difference approach.

Levich (4), Chao (5), and Moore (6) have employed boundary-layer theory to predict the flow around fluid spheres of low viscosity. The resulting drag coefficient equation is

$$C_D = \frac{48}{N_{Re}}\left(1 - \frac{2.2}{\sqrt{N_{Re}}}\right) \qquad (34)$$

A comparison of predicted drag coefficients with an experimental correlation for spherical bubbles after Tadaki and Maeda (*10*) is made in Table 2 ($C_D = 18.5/N_{Re}^{0.82}$). The agreement is good at Reynolds numbers of 50 and 100; the agreement with the finite-difference method at 200 is not particularly good. It is suggested that the radial and angular step sizes may be too large to describe accurately the flow at this large Reynolds number. Further work is being done to confirm this suspicion.

If reference is made to Figure 3 it is evident that the finite-difference solution approaches the potential flow solution as the Reynolds number is increased. At $N_{Re} = 200$ the potential flow solution agrees almost exactly with the finite-difference solution for polar angles as large as 90 deg. The difference in pressure in the vicinity of the rear stagnation point accounts for the fact that the form drag coefficient has a significant value. The form drag for potential flow is of course zero. Another point of interest is that the surface velocity distributions at $N_{Re} = 200$ are almost the same. For example, the finite-difference solution predicts a dimensionless velocity at the equator approximately equal to 1.3. Potential flow gives a velocity equal to 1.5. This suggests that for $N_{Re} \geq 200$ potential flow velocity distributions can be used to predict forced convection mass or heat transfer from circulating gas bubbles with reasonable accuracy.

CONCLUSION

It has been shown that finite-difference solutions may be used to predict accurately velocity distributions for viscous flow around circulating fluid spheres of low viscosity at intermediate Reynolds numbers. These profiles could now be used to predict forced convection heat or mass transfer. Finite-difference solutions have indicated that flow separation does not occur at $N_{Re} \leq 200$ for circulating fluid spheres of low viscosity. The accuracy of the boundary-layer theory after Levich-Chao-Moore has been confirmed. A new limiting analytical solution for creeping flow which accounts for the presence of an outer spherical

boundary at a finite distance from the sphere surface has been developed.

ACKNOWLEDGMENT

This study was supported by the National Research Council of Canada. W. T. Houghton received scholarships from the National Research Council. We appreciate the helpful suggestions of Vivien O'Brien.

LITERATURE CITED

1. Hadamard, J. S., *Compt. Rend.*, **152**, 1735 (1911).
2. Rybczynski, W., *Bull. Acad. Sci. Cracow*, **A40** (1911).
3. Hamielec, A. E., S. H. Storey, and J. M. Whitehead, *Can. J. Chem. Eng.*, **41**, 246 (1963).
4. Levich, V. G., *Z. Eksptl. Teoret. Fiz.*, **19**, 18 (1949).
5. Chao, B. T., *Phys. Fluids*, **5**, 69 (1962).
6. Moore, D. W., *J. Fluid Mech.*, **16**, 161 (1963).
7. Conkie, W. R., and P. Savic, *Natl. Res. Council (Canada) Rept. No. MT. 23* (1953).
8. Jenson, V. G., *Proc. Roy. Soc.*, **A249**, 346 (1959).
9. Satapathy, R., and W. Smith, *J. Fluid Mech.*, **10**, 561 (1961).
10. Tadaki, T., and S. Maeda, *Chem. Eng. (Tokyo)*, **2**, 254 (1961).

Manuscript received December 23, 1965; revision received July 14, 1966; paper accepted July 18, 1966.

The Forgotten Effect in Thermal Diffusion

WALTER J. KORCHINSKY and ALDEN H. EMERY, JR.

Purdue University, Lafayette, Indiana

The basic equations that describe the thermal diffusion column, including the forgotten effect, were solved numerically. When the density of the liquid in the column varies with concentration, the effect is important in transient batch operation of columns, increasingly so as the wall spacing decreases, but it has no influence at the steady state. Experimental work corroborated the theoretical results.

According to the theory, the instances of concentration reversal reported in the literature cannot be the result of the forgotten effect; the fluids involved could not have had the necessary properties. Attempted duplications of these instances in careful experiments yielded normal behavior. However, theoretical and experimental work on a column with a deliberately nonconstant wall spacing indicated that concentration reversals could occur in the complete absence of any forgotten effect contribution.

The basic theory of the thermal diffusion column, first presented in 1939 (*3, 5*), led to operating equations for the column that have been moderately successful in predicting the effects of the variables on the separations obtained in binary systems of liquids or gases, in both batch and continuous operation. One of the many simplifying assumptions made in these original derivations was that the density of the fluid used in the flow equation is a function of temperature only and not of concentration. In 1943, De Groot et al. (*4*) included the effect of concentration on density in an approximate way. Interest in the effect of concentration was really fired, however, when Prigogine et al. (*14*) in 1950 published a bizarre set of curves of concentration vs. time from batch operation of a column in which the difference in concentration between top and bottom started in one direction, slowed, and then went in the opposite direction, giving separations opposite from the original direction! This behavior, which we call *concentration reversal*, was attributed by them to the influence of concentration on density. Prigogine's article in French was accompanied by an abstract in English, in which *l'effèt oublié*, the term used by both De Groot and Prigogine for the hitherto *neglected* effect of concentration, was translated as the forgotten effect. Jones and Milberger (*8*) used this name in their 1953 article and the amusing appellation has stuck.

Since Prigogine's article, Jones and Milberger (*8*) and John and Bent (*7*) have observed concentration reversal (not to be confused with the forgotten effect), and these

Walter J. Korchinsky is with E. I. du Pont de Nemours Company, Inc., Wilmington, Delaware.